An Active Contour Model with Improved Shape Priors Using Fourier Descriptors*

D. Khuê Lê-Huu [1,2] **Fareed Ahmed** [1] **Julien Olivier** [2,1] **Romuald Boné** [2,1]
[1] Laboratoire d'Informatique, Université François–Rabelais, Tours, France
[2] École Nationale d'Ingénieurs du Val de Loire, Blois, France
huudienkhue.le@gmail.com, fareed.ahmed@etu.univ-tours.fr,
{julien.olivier, romuald.bone}@univ-tours.fr

Abstract

Snakes or active contours are widely used for image segmentation. There are many different implementations of snakes. No matter which implementation is being employed, the segmentation results suffer greatly in presence of occlusions, noise, concavities or abnormal modification of shape. If some prior knowledge about the shape of the object is available, then its addition to an existing model can greatly improve the segmentation results. In this work inclusion of such shape constraints for explicit active contours is presented. These shape priors are introduced through the use of Fourier based descriptors which makes them invariant to the translation, scaling and rotation factors and enables the deformable model to converge towards the prior shape even in the presence of occlusion and context noise. These shape constraints have been computed in descriptor space so no reconstruction is required and more generic descriptors can be used. Experimental results clearly indicate that the inclusion of these shape priors greatly improved the segmentation results in comparison with the original snake model.

1 Introduction

Active contours method was first introduced by Kass et al. (1988). In contrast to classical edge detection methods like Canny or Sobel filtering, where the resultant edge pixels may need some extra processing to form a connected contour, the active contour methods ensure that the contours are closed (there are open variants as well), connected and complete. These methods can generally be bifurcated into explicit (or parametric) active contours Kass et al. (1988) and implicit (or level set) methods Caselles et al. (1995). In explicit methods a deformable model is represented by a set of connected points that evolve dynamically to finally settle on contours in the image. However, such models are unable to automatically adapt to sudden topological changes. On the other hand, implicit active contours intrinsically adapts to any topology changes but at the same time embedding shape constraints in their evolution is not a straight forward process and thus increases complexity of the model.

When it comes to the implementation of snakes, many improvements have been proposed for both implicit and explicit models of active contours: finite elements methods Cohen and Cohen (1991), greedy algorithm Williams and Shah (1992), dynamic programming based solution Amini et al. (1990), active contours without edgesChan and Vese (2001), narrow band approaches Malladi et al. (1995) and Kim and Lee (2003).

In this work, the greedy algorithm was chosen because it provides an intuitive energy based explicit model for snakes. Thus, the inclusion of additional energy terms is a straightforward process. Likewise, the contour representation is well suited for shape based energy representation. The greedy

*In *International Conference on Computer Vision Theory and Applications* (VISAPP), pp. 472-476. 2013.

model is also cited by Kim and Lee (2003) for its stability and performance. Nevertheless, the segmentation results obtained from the explicit active contours are very sensitive to the initial position and parameters of the model and they suffer greatly in the presence of concave boundaries. These problems were addressed with the introduction of balloon force Cohen (1991) and Gradient Vector Flow (GVF) Xu and Prince (1998) in active contour model.

Regardless of the choice of implementation methods and their improvements, the segmentation results by active contours become highly inaccurate in the presence of occlusions, noise, object overlapping and extrusions. To address these issues and improve the segmentation results, the need for inclusion of some shape prior information in the segmentation process by active contours becomes quite evident. The literature suggests that some efforts have already been made in this regard. In diffusion snakes Caselles et al. (1995) a statistical shape knowledge is integrated into single energy functional. These shape statistics are derived from a set of binary training shapes. The curves are represented as a modified Mumford-shah functional. The shape energy is calculated based on Gaussian approximation of shape distribution. In affine Invariant Eigen snakes Xue et al. (2002), shape priors are embedded in the form of an internal energy term, which not only perform matching the deformable shape with template shape under affine transformations, but also performs local regularization to refine the fitting. It uses Bayesian framework and PCA to learn the main deformation modes from a set of template shapes. Such template matching schemes however, are sensitive to the shape and initialization of deformable template. In region based active contours, Legendre's moments are also used as shape priors Foulonneau et al. (2006). This is achieved by minimizing a distance between shape descriptors, defined by Legendre's moments, of a characteristic function.

Fourier based shape descriptors provide quite an efficient and powerful way of contour representation. Although such a representation can be particularly useful in the context of explicit active contours with shape priors, not much work has been done in this context. One such study proposes the representation of shape priors by elliptical Fourier descriptors Staib and Duncan (1992). Then, by using probabilistic approach, objects are associated to their respective classes and contour is converged towards the shape template belonging to that class. However, this method is too sensitive to parameters and initialization must be done very close to the goal shape to achieve the desired result. Most recently Fourier based geometric shape priors were used with the variational setup for snakes Charmi et al. (2008). Both the template and deformable model are represented by a set of Fourier descriptors. A force based approach is then used to guide the deformable contour towards the template by minimizing the difference between the reconstruction of template and deformable curve. The limit of this method is that it is not invariant to the starting point and needs the reconstruction of template and deformable contours in order to compute the force that guides the deformable model towards the template.

In this paper, a more improved version of snakes with Fourier based shape priors is presented. A more stable greedy implementation of snakes as well as a robust set of invariant Fourier descriptors are used for representation of active contours. More importantly, unlike the previous work, the shape matching is performed directly in the Fourier descriptor space rather than in the spatial domain, so there is no need for reconstruction of contours, which can improve significantly the computational speed. Moreover, a solution for automatic starting point invariance is presented to make the proposed method more robust and efficient.

When it comes to the quality of segmentation results, it is clear that some formal evaluation criteria is needed to validate the quality of a segmentation result. Such a quality measure can not only accurately interpret the segmentation results but can easily be used to compare different contour segmentation algorithms in general and those with shape priors in particular. Keeping this in mind, a state of the art method has been used to measure the quality of segmentation results obtained through our method.

This paper is organized as follows: section 2 provides an overview of the greedy approach for active contour model. In section 3, the prior shape representation and derivation of normalized Fourier descriptors is discussed. Section 4 presents our main contribution regarding the integration of Fourier based shape priors in active contour model. In section 5, experimental results are presented along with evaluation criteria for these results. Finally, in section 6, conclusions are drawn and perspectives are discussed.

2 Review of Snakes

In active contour method, the problem of edge detection is generally formulated as the energy minimization of a planner curve. The curve is denoted by $C(s,t) = (x(s,t), y(s,t))$ where t denotes the time and s the normalized arclength, $s \in [0,1]$.

The energy equation of such a curve contains basically two types of energy terms, namely internal energy E_{int} and external energy E_{ext}. The internal energy term is associated with geometrical properties of a parametric deformable curve. It essentially imposes constraints on the shape of the curve and controls stretching, bending or other intrinsic curve properties. These constraints depend on the type of internal energy being used and can be regulated with the associated parameters. Likewise, the external energy term is usually associated with the information present within the image itself. More generally, this term is associated with gradient information present in the image. In an ideal setup the total energy should converge to a local minimum at desired edges or boundaries. The total energy functional is given by

$$E_{\text{snake}} = \int_0^1 (E_{\text{int}} + E_{\text{ext}}) \mathrm{d}s \tag{1}$$

The *greedy algorithm* was chosen because of its energy based model. Indeed, in such a model inclusion of any additional energy term is quite intuitive. Similarly, curve representation is well suited for embedding shape based constraints as the energy minimization does not require complex mathematical formulations. This methods is also stable and, being an iterative approach, the solution is guaranteed. In greedy approach an initial contour is defined as a discrete closed curve with n vertices, each vertex is denoted by $v_i = (x_i, y_i)$ $(i = 0, 1, \ldots, n-1)$. x_i and y_i are the horizontal and vertical coordinates of each vertex. A given vertex v_i has its neighbours v_{i-1} and v_{i+1}. The discrete energy functional is defined as the sum of energies associated with each vertex, thus the greedy approach performs the global energy minimization by the means of successive local minimizations in a given window of fixed size w around each vertex. A discrete energy functional is computed for each of the neighbourhood pixels, say $\tilde{p}_i$, belonging to w and vertex v_i is moved to a location with minimum energy value. The equation for this discrete energy functional at each pixel $\tilde{p}_i \in w$ is given by

$$E(\tilde{p}_i) = E_{\text{int}}(\tilde{p}_i) + E_{\text{ext}}(\tilde{p}_i), \tag{2}$$

where $E_{\text{int}}(\tilde{p}_i)$ and $E_{\text{ext}}(\tilde{p}_i)$ are the discrete energy functional for internal and external energies. These generic internal and external energy terms can be replaced by any linear combination of internal and external energies along with their weight parameters.

Classically, only gradient based information is used as an external energy to guide the snake towards the edge features. This edge based energy is the inverse of the image gradient computed at each neighbourhood pixel $\tilde{p}_i$.

Gradient based information is very local. Thus, the active contour model usually fails to converge towards desired contour either if it is initialized far from the edges or in cases of concave boundaries, where edge based information may not be locally available. To avoid such problems, the Gradient Vector Flow (GVF) Xu and Prince (1998) provides an elegant solution by dispersing the edge information in the entire image to guide the active contour in the direction of strong edges, even in the presence of no or very little true edges in the locality. The GVF, however, is a forced field based solution. To apply a similar energy as GVF in the greedy setup, a distance transform has been used. The distance transform is generally calculated by computing an edge map of an image and transforming each pixel position into a distance from its nearest edge. In principal, the distance matrix and edge calculation method may vary in different implementations. In literature, Svensson and Borgefors (2002) and Fabbri et al. (2008) presented good surveys and comparisons of different distance transform techniques.

The Distance Transformed based energy term is given by

$$E_{\text{dt}}(\tilde{p}_i) = DT(\tilde{p}_i), \tag{3}$$

where $DT(\tilde{p}_i)$ is the distance transform value of the pixel $\tilde{p}_i$. This energy term will be referred as gradient distance flow, which attains its minimum value nearer to the contour points.

In this work, the continuity, curvature and balloon energies will be used as internal energy components. The continuity energy controls the stretching and makes sure that the control points are equally spaced,

while the curvature energy enforces smoothness and avoid oscillations of the snake by penalizing high contour curvatures. Besides, the balloon energy helps the deformable model to expand or contract in the direction of the normals of the curve (depending on the sign of an associated parameter). A greedy derivation of balloon energy term Mille et al. (2006) was used in our implementation.

Finally, the equation for a discrete energy functional incorporating all these energy terms, along with their associated weights is given by

$$E(\tilde{p}_i) = \alpha E_{\text{cont}}(\tilde{p}_i) + \beta E_{\text{curv}}(\tilde{p}_i) + \gamma E_{\text{ball}}(\tilde{p}_i) + \delta E_{\text{dt}}(\tilde{p}_i), \tag{4}$$

where $E_{\text{cont}}(\tilde{p}_i), E_{\text{curv}}(\tilde{p}_i), E_{\text{ball}}(\tilde{p}_i), E_{\text{dt}}(\tilde{p}_i)$ are respectively the energy terms for continuity, curvature, balloon energy, distance transform and $\alpha, \beta, \gamma, \delta$ are their associated weights.

The next section provides a detailed discussion about the invariant Fourier descriptors, which will be used to derive the shape based energy term.

3 Fourier based invariant shape descriptors for Snakes

Fourier descriptors are well known for their ability to provide a compact representation for contours or shape outlines. Furthermore, these descriptors can easily be normalized to make the contour matching process invariant to translation, rotation and scaling factors. Fourier descriptors are also known to be robust to noise. The use of these descriptors is quite appropriate in case of explicit active contours, since the curve is already defined as outline with fixed number of control points, which makes the derivation of these descriptors straighforward. Moreover, in this work the reference shape is also represented in the similar manner. Therefore, the invariant properties of Fourier descriptors are well suited for its representation as well.

In order to derive the invariant Fourier descriptors for a shape, an appropriate representation has to be chosen. Suppose that the shape is represented by a discrete closed curve of n vertices $v_i = (x_i, y_i)$ $(i = 0, 1, \ldots, n-1)$. A complex mapping was used as suggested by Charmi et al. (2008) and Bartolini et al. (2005) to represent these coordinates in complex form as: $z_i = x_i + j \cdot y_i$.

The Discrete Fourier Transform (DFT) of z_i is given by a set of Fourier coefficients

$$Z_k = \sum_{i=0}^{n-1} z_i e^{-j\frac{2\pi i k}{n}} \quad \text{for } k = -\frac{n}{2}, \ldots, \frac{n}{2} - 1. \tag{5}$$

The above DFT can also be represented as

$$Z_k = R_k e^{j\theta_k}, \tag{6}$$

where R_k is known as amplitude (or modulus) and θ_k as phase.
The normalized descriptors

$$\hat{Z}_k = \hat{R}_m e^{j\hat{\theta}_m}, k = -\frac{n}{2}, \ldots, \frac{n}{2} - 1, \tag{7}$$

having the following properties are translation-, scale- and rotation-invariant (but not starting point-invariant), as proved by Bartolini et al. (2005):

$$\hat{Z}_0 = 0, \tag{8}$$

$$\hat{R}_k = \frac{R_k}{R_1} \quad (k \neq 0), \tag{9}$$

$$\hat{\theta}_k = \theta_k - \theta_1 \quad (k \neq 0). \tag{10}$$

From this set of invariants, we can reconstruct the (normalized) shape using the Inverse Discrete Fourier Transform (iDFT):

$$\hat{z}_i = \frac{1}{n} \sum_{k=-n/2}^{n/2-1} \hat{Z}_k e^{j\frac{2\pi i k}{n}} \quad \text{for } i = 0, 1, \ldots, n-1. \tag{11}$$

In this paper, this will be called *reconstructed shape*. The reconstructed shape of a curve C will be denoted $\hat{C}$.

4 Embedding shape prior into snakes

4.1 Shape prior energy

To introduce shape prior information, a prior energy term is added to the energy functional of the snake.

Let C_{ref} be a template contour describing a shape. This contour has n vertices $v_i^{\text{ref}} = (x_i^{\text{ref}}, y_i^{\text{ref}})$ $(i = 0, 1, \ldots, n-1)$ (practically, n is chosen depending on the complexity of the shape). Now for a contour C having the same size, $v_i = (x_i, y_i)$ $(i = 0, 1, \ldots, n-1)$, the prior term has to constrain it to evolve to a shape similar to the given template.

As described in the previous section, the reconstructed shapes $\hat{C}_{\text{ref}}$ and $\hat{C}$ can be obtained using the normalized Fourier descriptors. The prior energy can be defined as the *distance* between $\hat{C}_{\text{ref}}$ and $\hat{C}$: the smaller this distance is, the more similar to the reference shape the contour will be.
Several methods of distance measuring can be used. The choice of an appropriate method will be discussed later in this section. For now, let $D(a,b)$ denote the distance (in general) between a et b. Then, the shape prior energy of a snake C regarding a reference shape C_{ref} can be defined as

$$E_{\text{prior}}(C) = D(\hat{C}, \hat{C}_{\text{ref}}). \tag{12}$$

For integrating this energy into the discrete energy functional of the snake, we need its discrete form. For a neighboring pixel $\tilde{p}_i$ of a vertex v_i $(i = 0, 1, \ldots, n-1)$, a new curve C_i is considered by simply replacing the vertex v_i by $\tilde{p}_i$. The shape prior energy of the pixel $\tilde{p}_i$ is then defined as

$$E_{\text{prior}}(\tilde{p}_i) = D(\hat{C}_i, \hat{C}_{\text{ref}}). \tag{13}$$

The global energy function of the snake can be now written as

$$E(\tilde{p}_i) = \alpha E_{\text{cont}}(\tilde{p}_i) + \beta E_{\text{curv}}(\tilde{p}_i) + \gamma E_{\text{ball}}(\tilde{p}_i) + \delta E_{\text{dt}}(\tilde{p}_i) + \zeta E_{\text{prior}}(\tilde{p}_i). \tag{14}$$

Now, as mentioned previously, let us discuss about an appropriate method of calculating the distance between $\hat{C}_i$ and $\hat{C}_{\text{ref}}$. Besides the classical Euclidean distance, different methods have been developed in the literature. Many of these have been proved to be working by our own implementation, such as the generic discrepancy measure Cardoso and Corte-Real (2005) or the Pratt criterion for evaluating segmentations Pratt et al. (1978) (see also section 5.2, page 9), and especially the Dynamic Time Warping distance, which has a huge advantage in comparison with the others: allowing elastic shiftings of the time axis, e.g. to accommodate signals which are similar, but where a phase difference between some samples exists Keogh (2002). However, the Euclidean distance has been proved to be the most effective in terms of computation efficiency, as explained thereafter.

Although the greedy algorithm is known for its rapidity, the integration of such distance calculation has decreased significantly its performance. Indeed, at each iteration of the algorithm, for each vertex of the snake, the DFT and iDFT are performed for each of the neighboring pixels. If n is the size of the snake and $m \times m$ is the size of the neighborhood, then the DFT and iDFT are performed $n \cdot m^2$ times at each iteration, while these last ones themselves need a lot of computation already.

Fortunately, by using the Euclidean, we can avoid performing the iDFT, thanks to Parseval's theorem, stating that *the sum of the square of a function is equal to the sum of the square of its transform*. Indeed, if $\hat{Z}_k, \hat{Z}_k^{\text{ref}}$ $(k = -\frac{n}{2}, \ldots, \frac{n}{2} - 1)$ denote the normalized descriptors and $\hat{z}_i, \hat{z}_i^{\text{ref}}$ $(i = 0, 1, \ldots, n-1)$ the reconstructed shapes of the snake and the reference shape, respectively, then the Euclidean distance based shape prior energy can be rewritten as (*ED* for Euclidean distance)

$$E_{\text{prior}}(C) = ED(\hat{C}_i, \hat{C}_{\text{ref}}) = \sqrt{\sum_{i=0}^{n-1} |\hat{z}_i - \hat{z}_i^{\text{ref}}|^2} = \sqrt{\sum_{k=-n/2}^{n/2-1} |\hat{Z}_k - \hat{Z}_k^{\text{ref}}|^2}. \tag{15}$$

A solution to overcome the limits of the Euclidean metric in accommodating phase differences between similar shapes will be discussed later in the next section.

4.2 Snake's evolution with shape prior

In the beginning of the evolution, the snake does not have any information about the object to be segmented, so the prior energy will attract it to the reference shape but in the way that has no reason

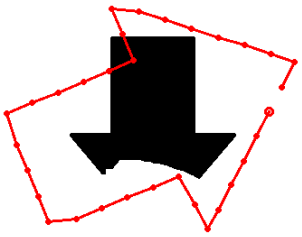

Figure 1: A final snake under prior force only (the initial snake is a circle outside the object).

to be related to the object. The Figure 1 is an example of a snake under the prior force only. It can be noted that, with just only the prior energy, the snake will have difficulty converging to the desired contour. To overcome this problem, the following strategy was adopted:

In the beginning, the shape prior weight should be very small as compared to the other weights, so that the snake can evolve freely from (or under little effect of) the shape prior constraint. This will allow it to capture parts of the object's contour.

Now that the snake has some information about the object, it should know how to evolve to the prior shape next. The prior weight should now increase gradually as compared to the other weights, or equivalently, the other weights should decrease gradually as compared to the prior weight. This led us to the idea of modifying slightly the above model of snake: the weight parameters are function of time and may vary dynamically ($\alpha \to \alpha(t), \beta \to \beta(t)$, etc...). In particular, in our method, it suffices to define the prior weight (i.e. ζ) as a strictly increasing function of time and the others as constants. For $\zeta(t)$, we observed that the linear function is efficient: $\zeta(t) = k \cdot t$ ($k > 0$). In addition, to prevent this weight from increasing infinitely and beginning too big as compared to the other weights, a threshold value $\zeta_{\max}$ is set as well:

$$\zeta(t) = \begin{cases} k \cdot t & \text{if } k \cdot t \leq \zeta_{\max} \\ \zeta_{\max} & \text{if } k \cdot t > \zeta_{\max}. \end{cases} \tag{16}$$

Finally, the energy functional can be rewritten as

$$E = \alpha E_{\text{cont}} + \beta E_{\text{curv}} + \gamma E_{\text{ball}} + \delta E_{\text{dt}} + \zeta(t) E_{\text{prior}}, \tag{17}$$

where $\zeta(t)$ is defined as in the equation (16) (in our implementation, t is the iteration number of the algorithm, as an iteration can represent a unit of time).

It remains a problem with the Euclidean distance. Let us take the above example of the arrow. The Figure 2a shows a snake that has successfully captured the contour of the object. From this snake, if we apply the prior energy only, then it will evolve to its final state as shown in Figure 2b. We

(a) (b)

Figure 2: The snake in (a) evolves to the final snake in (b), under shape prior constraint using Euclidean distance.

can observe that the prior constraint forces the snake to converge well to something similar to the reference shape. However, in the same time, it also tries to rotate the snake, and so the snake will hardly evolve to the desired contour. This is because there is a difference in phase between the constructed shape of the snake and the one of the reference shape. As mentioned earlier, the limit of the Euclidean distance is not allowing to accommodate phase differences between similar shapes.

Therefore, by minimizing the shape prior energy, the snake is forced to rotate such that the above phase difference is reduced.

To overcome this problem, we propose to minimize the phase difference between the constructed shapes before the prior energy takes effect, without translating, rotating or scaling the snake, of course.
As the descriptors used are not starting point-invariant, it is obvious that if we change the starting point of the snake, the phase of the constructed shape is also changed. This leads us to the idea of shifting the starting point to the point for which the phase difference is minimal. This step is called the *starting point correction*. In practice, we use the Euclidean distance $DE(\hat{C},\hat{C}_{\text{ref}})$ itself for calculating approximatively the phase difference.
The starting point correction should be performed many times during the running of the snake to ensure a good evolution, for example at each fixed number of iterations. Practically, in our implementation, we observed that it can be performed at every iteration without any noticeable time consumption.

To sum up, below is the greedy algorithm of our method. $\hat{C}$ and $\hat{C}_{\text{ref}}$ are the constructed shape of the snake and the reference shape, respectively.

1. For each vertex v_i of the snake, $i = 0, 1, \ldots, n-1$, search its neighborhood to find the location that minimizes the energy functional. Move v_i to that location.
2. Once 1. has finished with all the n vertices (i.e. 1 iteration), shift the starting point of the snake to the one that minimizes the phase difference between the constructed shape of the snake and the one of the reference shape, i.e. $\hat{C}$ and $\hat{C}_{\text{ref}}$. Update the value of $\zeta(t)$.
3. Repeat steps 1 and 2 until only a very small fraction of snake points move in an iteration.

5 Experimental results

We observed that with our prior based constraint setup, the snakes need only the continuity, the distance transform and the prior terms to work properly on many test images. In all experiments presented below, we used the following parameters:

$$\alpha = 1, \beta = \gamma = 0, \delta = 1 \tag{18}$$

and the weight $\zeta(t)$ of the prior energy is defined as in the equation (16) where k and $\zeta_{\max}$ may vary for different shapes and/or different images.

Experiments with both synthetic image and real images are utilized to demonstrate the performance of our method. The results are compared with the classical snakes without any prior term. Moreover, as in applications where the accuracy of segmentation results is of high priority, merely visually satisfactory results may not be a good criterion for evaluation, so a more sophisticated and qualitative metric is required to evaluate the quality of the segmentations with respect to some ground truth. A comparative study of main evaluation criteria is proposed by Chabrier et al. (2004) and the Pratt criterion Pratt et al. (1978) (also called Figure of Merit) is identified as the most effective. This last corresponds to the empirical distance between the set of boundaries Ω_G from the ground truth and the set of boundaries Ω_S from the segmented image:

$$P(\Omega_G, \Omega_S) = \frac{\sum_{i=1}^{\text{card}(\Omega_S)} \frac{1}{1+d_i(\Omega_S,\Omega_G)^2}}{\max\{\text{card}(\Omega_S), \text{card}(\Omega_S)\}}, \tag{19}$$

where $d_i(\Omega_S, \Omega_G)$ is the distance between the i$^{\text{th}}$ pixel of Ω_S and its closest pixel in Ω_G. Furthermore, $P(\Omega_G, \Omega_S) = 1$ indicates perfect segmentation result, while its reduced values specifies poor segmentation results.

We will use this criteria for our evaluation of the results.

5.1 Synthetic images

The Figure 3 shows images of two different objects with the original snakes: an arrow occluded by another shape and a cross with a part missing. The reference shapes are shown in Figure 4.

Figure 3: Synthetic images with initial snakes.

Figure 4: Reference shapes.

Without the prior term, the snakes cannot properly segment the objects despite successfully capturing their contours, as shown in Figure 5. On the contrary, by adding the prior energy, we can see that the snakes have succesfully converged to the desired boudaries (Figure 6).

Figure 5: Results without shape prior.

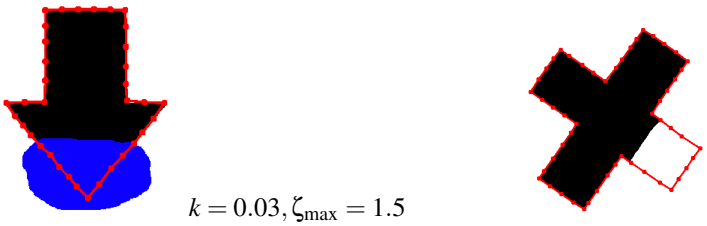

$k = 0.03, \zeta_{\max} = 1.5$ $k = 0.05, \zeta_{\max} = 2.5$

Figure 6: Results with shape prior.

For a numerical evaluation, the ground truths for these examples were easily calculated from original images (with no occlusion and missing parts). The segmentation results are compared in Table 1 using Pratt criterion.

With shape prior, the results are clearly more precise.

Results for only some particular values of k and $\zeta_{\max}$ have been presented, but through many experiments, we observed that the method can work with a large range of these two parameters. For example, in the both experiments above, if $k = 0.05$ and $\zeta_{\max}$ is equal to any value between 1.2 and 2.5 then we will obtain very similar results. In general, $\zeta_{\max}$ may vary between 1.0 and 3.0, and k may vary between 0.01 and 0.1 (the other parameters are set according to the equation (18)). Yet, the value of k depends on how the snake is initialized: the farther the initial snake is from the object's

Table 1: Comparison of segmentation results on synthetic images (values are multiplied by 10^2).

Image	Without shape prior	With shape prior
Arrow	28.09	**82.86**
Cross	20.64	**85.03**

contour (e.g. the initial snake is too big or too small), the smaller k should be (as the snake needs more time to capture parts of the object's contour, the prior term should increase more slowly (see explanation in Section 4, page 5), which means k is smaller).

5.2 Real images

To further test the efficiency of the method, our next expriments are carried out on real images.

The image in Figure 7a shows a telephone occluded by a hand. The reference shape we used is given in Figure 7b. In Figure 7a, the initial snake (red line) and the ground truth (blue line) are also presented. The segmentation results are presented in Figure 8, where we used $k = 0.03$ and $\zeta_{\max} = 1.5$. The Pratt values are presented in Table 2.

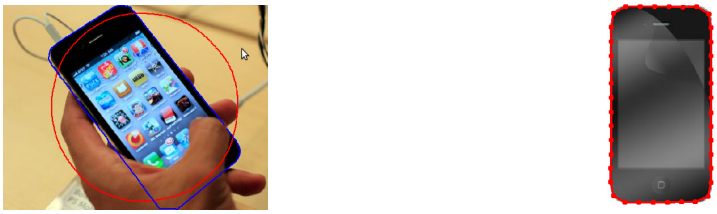

(a) (b)

Figure 7: (a) Image with initial snake and ground truth and (b) reference shape.

(a) Without shape prior (b) With shape prior

Figure 8: Image with initial snake (a) and reference shape (b).

We proceed with some more difficult images (the gradient map is more complex).

For the examples of boletus presented in Figure 10, the reference shape presented in Figure 9 is used. This contour was created by taking some image samples of boletuses, extracting their contours and then taking the mean contour of all the extracted ones. The initial snakes and the ground truth are also presented in Figure 10. The results are presented in Figure 11) where we used $k = 0.03, \zeta_{\max} = 1.5$ for the first case and $k = 0.02, \zeta_{\max} = 1.2$ for the second case. Finally, these results are evaluated numerically in Table 2. Again, it is clear that the results are more precise with shape priors.

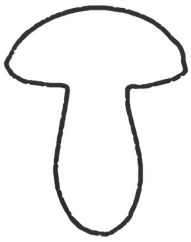

Figure 9: Reference shape for boletus example.

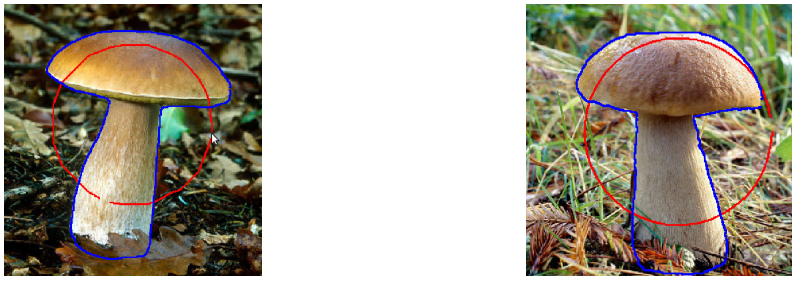

(a) Boletus 1 (b) Boletus 2

Figure 10: Boletus images with initial snakes (red lines) and ground truth (blue lines).

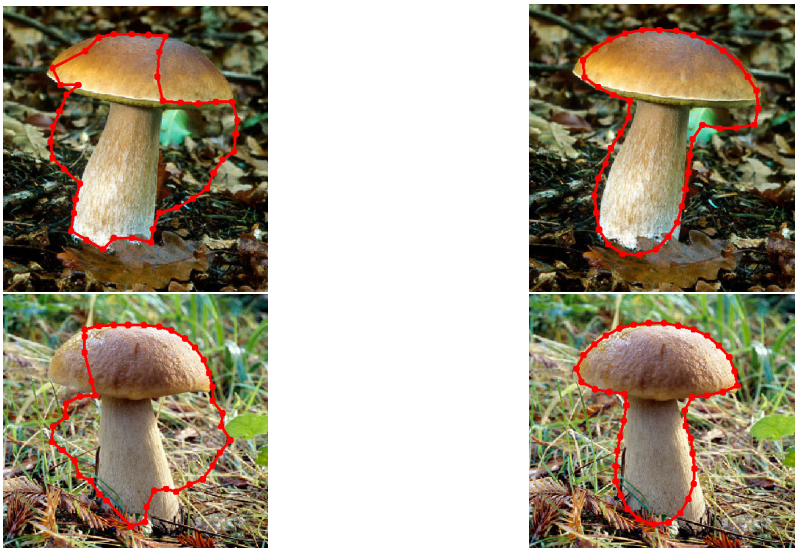

(a) Without shape prior (b) With shape prior

Figure 11: Results on boletus test.

Table 2: Comparison of segmentation results on real images (values are multiplied by 10^2).

Image	No shape prior	Shape prior
Telephone	16.09	**46.85**
Mushroom 1	10.08	**12.40**
Mushroom 2	13.69	**15.96**

Next, we will take an example for comparing our method with another state-of-the-art method of segmentation with shape priors.

The images in Figure 14 were segmented by a shape prior method using the distance-based shape statistics (DBSS) Charpiat et al. (2007). Using our method, we get the results shown in Figure 15. The results using the classical snake (no shape prior) are also presented in Figure 13.

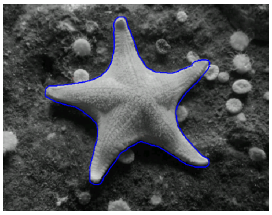

Figure 12: Ground truth (blue line) for the starfish image.

Figure 13: Results without shape prior.

Figure 14: Results with shape prior by DBSS.

Figure 15: Results with shape prior by our method.

Visually, it is clear that without any shape prior, the snake gives very bad results. For the two methods with shape prior, it is difficult to tell which one is better than the other. Now using Pratt Critation as before, the evaluation of segmention results are presented Table 3.

Table 3: Comparison of segmentation results (values are multiplied by 10^2).

Image	No prior	DBSS	Our method
Non-occluded	5.92	23.53	**29.00**
Occluded	3.24	12.57	**13.62**

We can see that our method has a relatively good performance.

6 Conclusions

In this paper, a new model with translation, scale, rotation and starting point invariant shape priors for explicit active contour has been presented. Calculation of shape based energy was entirely performed in the descriptors space, i.e. there is no need to reconstruct the prior shape during evolution of active contours, which is a gain in terms of computation time. Visual and numerical evaluations on both synthetic and real images have shown that our method greatly improves the segmentation results, even in presence of occlusion and incomplete shapes.

In the near future, we would also like to test our method on video data. The implementation for the level set method will be considered as well.

References

Amini, A. A., Weymouth, T. E., and Jain, R. C. (1990). Using dynamic programming for solving variational problems in vision. *IEEE Transactions on Pattern Analysis and Machine Intelligence*, 12(9):855–867.

Bartolini, I., Ciaccia, P., and Patella, M. (2005). Warp: Accurate retrieval of shapes using phase of fourier descriptors and time warping distance. *IEEE Transactions on Pattern Analysis and Machine Intelligence*, 27(1):142–147.

Cardoso, J. S. and Corte-Real, L. (2005). Toward a generic evaluation of image segmentation. *IEEE Transactions on Image Processing*, 14(11):1773–1782.

Caselles, V., Kimmel, R., and Sapiro, G. (1995). Geodesic active contours. *International Journal of Computer Vision*, 22(1):61–79.

Chabrier, S., Laurent, H., Emile, B., Rosenberger, C., and Marché, P. (2004). A comparative study of supervised evaluation criteria for image segmentation. *EUSIPCO 04*, pages 1143–1146.

Chan, T. F. and Vese, L. A. (2001). Active contours without edges. *IEEE transactions on image processing*, 10(2):266–277.

Charmi, M. A., Derrode, S., and Ghorbel, F. (2008). Fourier-based geometric shape prior for snakes. *Pattern Recognition Letters*, 29(7):897–904.

Charpiat, G., Faugeras, O. D., and Keriven, R. (2007). Shape statistics for image segmentation with prior. In *CVPR*.

Cohen, L. D. (1991). On active contour models and balloons. *CVGIP: Image Understanding*, 53(2):211–218.

Cohen, L. D. and Cohen, I. (1991). Finite element methods for active contour models and balloons for 2d and 3d images. *IEEE Transactions on Pattern Analysis and Machine Intelligence*, 15:1131–1147.

Fabbri, R., Costa, L. D. F., Torelli, J. C., and Bruno, O. M. (2008). 2d euclidean distance transform algorithms: A comparative survey. *ACM Computing Surveys*, 40(1):2:1–2:44.

Foulonneau, A., Charbonnier, P., and Heitz, F. (2006). Affine-invariant geometric shape priors for region-based active contours. *IEEE Transactions on Pattern Analysis and Machine Intelligence*, 28(8):1352–1357.

Kass, M., Witkin, A., and Terzopoulos, D. (1988). Snakes: Active contour models. *International Journal of Computer Vision*, 1(4):321–331.

Keogh, E. (2002). Exact indexing of dynamic time warping. In *Proceedings of the 28th international conference on Very Large Data Bases*, VLDB '02, pages 406–417. VLDB Endowment.

Kim, C.-T. and Lee, J.-J. (2003). An active contour model for object tracking using the previous contour. *Artificial Life and Robotics*, 7:6–11.

Malladi, R., Sethian, J. A., and Vemuri, B. C. (1995). Shape modeling with front propagation: A level set approach. *IEEE Transactions on Pattern Analysis and Machine Intelligence*, 17(2):158–175.

Mille, J., Boné, R., Makris, P., and Cardot, H. (2006). Greedy algorithm and physics-based method for active contours and surfaces: A comparative study. In *ICIP*, pages 1645–1648. IEEE.

Pratt, W. K., Faugeras, O. D., , and Gagalowicz, A. (1978). Visual discrimination of stochastic texture fields. *IEEE Transactions on Systems, Man, and Cybernetics*, 8(11):796–804.

Staib, L. H. and Duncan, J. S. (1992). Boundary finding with parametrically deformable models. *IEEE Transactions on Pattern Analysis and Machine Intelligence*, 14(11):1061–1075.

Svensson, S. and Borgefors, G. (2002). Digital distance transforms in 3d images using information from neighbourhoods up to 5x5x5. *Computer Vision and Image Understanding*, 88(1):24–53.

Williams, D. J. and Shah, M. (1992). A fast algorithm for active contours and curvature estimation. *CVGIP: Image Understanding*, 55(1):14–26.

Xu, C. and Prince, J. L. (1998). Snakes, shapes, and gradient vector flow. *IEEE Transactions on Image Processing*, 7(3):359–369.

Xue, Z., Li, S. Z., and Teoh, E. K. (2002). Ai-eigensnake: an affine-invariant deformable contour model for object matching. *Image and Vision Computing*, 20(2):77–84.